Bull. Chem. Soc. Jpn., 64, 3511—3514 (1991)

# Solvent Effect on the ESR Parameters of Di-*t*-butyl Nitroxide and Galvinoxyl. Theoretical Application of the MNDO Effective Charge Model

Hideto Takase, Kenji Morihashi, and Osamu Kikuchi*
Department of Chemistry, University of Tsukuba, Tsukuba 305
(Received May 30, 1991)

An effective charge model of the solvent effect was incorporated with the RHF-MNDO-CI method for free radicals, allowing the solvent effect on the hyperfine coupling constants (hfcc) and *g*-values of the di-*t*-butyl nitroxide (DTBN) and galvionxyl radicals to be examined. The calculated solvent dependences of the spin distribution and the n→π* excitation energy of DTBN have well elucidated the observed solvent effect on the hfcc and *g*-value of DTBN. The observed trend for the proton hfcc of galvinoxyl has been correctly reproduced by the present theoretical model.

The hyperfine coupling constants (hfcc) and *g*-value derived from the ESR spectra of a free radical vary with the solvent polarity; the solvent dependences of these ESR parameters have been considered theoretically.[1–4] Among the various theoretical models concerning the solvent effect, the effective charge model is one of the continuum models based on Born's solvation energy.[5] This model was first suggested by Klopman,[6] and a correct description has been given by Tapia[7] as well as by Constanciel and Contreras.[8] In our previous papers, the MNDOS method, in which the effective charge model is incorporated with the MNDO[9] method, was proposed and applied to a conformational analysis of both amine[10] and amino acids in solution,[11] as well as the solvent effect on the potential energy surface of typical $S_N2$ reactions.[12] In this paper we extend the MNDOS method to an open-shell RHF method for free radicals. The solvent effect was also introduced to the configulation interaction (CI) calculation, and the RHF-MNDOS-CI method was applied in order to examine the solvent effect on the hfcc and *g*-value of typical neutral free radicals, di-*t*-butyl nitroxide (DTBN) and galvinoxyl radicals.

## Experimental

DTBN and galvinoxyl were purchased commercially and were used as received. The spectrograde solvents were dried on 3 or 4 Å molecular sieves which were activated before use. The dried solvents were transferred into the sample tube in the vacuum line. Fremy salt was used as the standard sample; the nitrogen hfcc and *g*-value are 13.00 G (1 G=$10^{-4}$ T) and 2.00550, respectively.

## Method of Calculation

In a previous paper[13] we reported that the RHF-MNDO-CI method gives better agreement with experiments than does the UHF-MNDO method in calculations concerning hfcc of $\pi$-radicals. In this paper the effective charge model is incorpolated with the RHF-MNDO-CI method in order to evaluate the solvent effect on the ESR parameters of $\pi$-radicals.

In the effective charge model, the solvation energy is given by a generalized Born formula, which was derived by Hoijtink et al.[14] as well as Chalvet and Jano:[15]

$$E^{\mathrm{solv}}=-\frac{1}{2}(1-\varepsilon^{-1})\sum_{\mathrm{A}}Q_{\mathrm{A}}^{2}/r_{\mathrm{A}}-\frac{1}{2}(1-\varepsilon^{-1})\sum_{\mathrm{A}}\sum_{\mathrm{B}}Q_{\mathrm{A}}Q_{\mathrm{B}}/R_{\mathrm{AB}}. \tag{1}$$

Here, A and B are atoms in the molecule, $Q_{\mathrm{A}}$ and $r_{\mathrm{A}}$ are the charge and the radius of the A atom, respectively, and $R_{\mathrm{AB}}$ is the distance between A and B. The energy of a free radical in solution ($E^{\mathrm{S}}$) is the sum of the energy in its isolated state ($E^0$) and the solvation energy ($E^{\mathrm{solv}}$):

$$E^{\mathrm{S}}=E^0+E^{\mathrm{solv}}. \tag{2}$$

$E^0$ is calculated using the restricted wavefunction for the doublet state:

$$\Psi_g=|\phi_1\bar{\phi}_1\cdots\phi_{m-1}\bar{\phi}_{m-1}\phi_m>. \tag{3}$$

Since the atomic population is derived under the ZDO approximation using semiempirical MO methods, the variational procedure for the solvation energy term (Eq. 1) was carried out under the ZDO approximation. The variational method gives two Fock operators ($F^{\mathrm{c}}$ and $F^{\mathrm{o}}$) for a doubly-occupied MO and a singly-occupied MO, respectively:

$$F^{\mathrm{c}}=H_{\mathrm{core}}+\sum_{l}(2J_l-K_l)+\frac{1}{2}(2J_m-K_m)+G$$

and

$$F^{\mathrm{o}}=\frac{1}{2}[H_{\mathrm{core}}+\sum_{k}(2J_k-K_k)+G]. \tag{4}$$

The *G* term is an additional operator which reflects the solvent effect:

$$G=-(1-\varepsilon^{-1})(2\sum_{l}J_l+J_m-L)$$

and

$$L=\left[\sum_{\mathrm{B}}Z_{\mathrm{B}}\int d\tau_2\chi_{\mathrm{B}}^{*}(2)\frac{1}{r_{12}}\chi_{\mathrm{B}}(2)\right], \tag{5}$$

where $Z_{\mathrm{B}}$ is the core charge and $\chi$ are the atomic orbitals. The matrix elements of *G* with respect to atomic orbitals are

$$G_{rr}=<\chi_r|G|\chi_r>=(1-\varepsilon^{-1})\sum_{\mathrm{B}}Q_{\mathrm{B}}\Gamma_{\mathrm{AB}}$$

and

$$G_{rs} = <\chi_r|G|\chi_s> = 0, \tag{6}$$

where $\Gamma_{AB}$ are the electron repulsion integral and are evaluated by an empirical formula.[12] The off-diagonal elements for $G$ are zero, due to the ZDO approximation. Two Fock operators ($F^c$ and $F^o$) were unified and solved according to the general SCF procedure by Hirao and Nakatsuji.[16]

In the CI calculation, only one type of singly-excited configuration function ($\Psi_{i\rightarrow k}$(II)) which mixes directly with $\Psi_g$, was included,[13]

$$\begin{aligned}\Psi_{i\rightarrow k}(\mathrm{II}) = \frac{1}{\sqrt{6}}\Big\{&|\cdots\phi_i\bar{\phi}_k\cdots\phi_{m-1}\bar{\phi}_{m-1}\phi_m> \\ &-|\cdots\phi_k\bar{\phi}_i\cdots\phi_{m-1}\bar{\phi}_{m-1}\phi_m> \\ &-2|\cdots\phi_i\phi_k\cdots\phi_{m-1}\bar{\phi}_{m-1}\bar{\phi}_m>\Big\}.\end{aligned} \tag{7}$$

The CI matrix elements were calculated for the following operator:

$$H^S = H + \sum_i G(i), \tag{8}$$

where $H$ is the Hamiltonian for an isolated molecule and $G(i)$ is an one-electron operator for the solvent effect. The matrix elements for $G(i)$ with respect to the MO's are related to $G_{rr}$ in Eq. 6 by

$$<\phi_i|G|\phi_j> = \sum_r C_{ri}C_{rj}G_{rr}, \tag{9}$$

where $C_{ri}$ and $C_{rj}$ are the LCAO coefficients.

The hfcc were calculated using the following equation:[17]

$$a_A = (8\pi/3)g_e\beta_e\hbar\gamma_A|\chi_S^{(A)}(0)|^2\rho_S^{(A)}, \tag{10}$$

where $\rho_S^{(A)}$ is the spin density of the s-type valence atomic orbital on atom A calculated using the CI wavefunction; the others are constants for the electron and the atom.

The $g$-value was obtained as an average of three principle values of a $g$-tensor, which were calculated using Stone's equation:[18]

$g_{\mu\nu} = g_e\delta_{\mu\nu} + \Delta g_{\mu\nu}$, where

$$\begin{aligned}\Delta g_{\mu\nu} = &\sum_{i=1}^{m-1} 2<\phi_i|\sum_A L_\mu^{(A)}|\phi_m><\phi_m|\sum_A \xi^{(A)}L_\nu^{(A)}|\phi_i>/\Delta E_{i\rightarrow m} \\ &-\sum_{k=m+1}^{n} 2<\phi_m|\sum_A L_\mu^{(A)}|\phi_k><\phi_k|\sum_A \xi^{(A)}L_\nu^{(A)}|\phi_m>/\Delta E_{m\rightarrow k}.\end{aligned} \tag{11}$$

Here, $\phi_i$ and $\phi_k$ are the doubly-occupied and vacant MO obtained by the RHF-MNDOS method, respectively. In this equation, the one-electron excitation energy should be evaluated for a Hamiltonian which includes the solvent effect:

$$\Delta E_{i\rightarrow m} = <\Psi_{i\rightarrow m}|H^S|\Psi_{i\rightarrow m}> - <\Psi_g|H^S|\Psi_g>$$

and

$$\Delta E_{m\rightarrow k} = <\Psi_{m\rightarrow k}|H^S|\Psi_{m\rightarrow k}> - <\Psi_g|H^S|\Psi_g>. \tag{12}$$

In this way, an effective charge model has been introduced into both the open-shell RHF-MNDO method and the CI calculation, allowing the solvent effect on the ESR parameters to be evaluated.

## Results and Discussion

**DTBN.** The solvent dependence of the hfcc and $g$-value of DTBN are listed in Table 1. Since the electronic structure of a free radical is affected by the various properties of the solvent, it may be difficult to rationalize the observed solvent dependence of the ESR parameters by any single property of the solvent. However, Table 1 shows clear trends between the ESR parameters of DTBN as well as the dielectric constant of the solvent; the hfcc of the nitrogen atom increases with an increase in the dielectric constant of the solvent ($\varepsilon$), while the $g$-value decreases with an increase in $\varepsilon$. These trends are characteristic of nitric oxide radicals.[4]

In the MO calculation, the $t$-butyl groups in DTBN were replaced by methyl groups and assumed to have $C_{2v}$ symmetry (Fig. 1). The geometry was optimized by the RHF-MNDOS method for several $\varepsilon$ values.

The computational results are shown in Table 2. The nitrogen hfcc ($a_N$) increases with an increase in $\varepsilon$, while the $g$-value decreases with an increse in $\varepsilon$. These trends were observed in experiments (Table 1). An analysis of the electronic structure of DTBN reveals the essential feature of the solvent dependence of the hfcc and $g$-value. The calculated net charges of the nitrogen and oxygen ($Q_N$ and $Q_O$) are shown in Table 2. As can be seen from Table 2, $Q_O$ becomes more negative and $Q_N$

Table 1. Experimental hfcc and $g$-Values of DTBN in Various Solvents

| Solvent | $\varepsilon$ | $a_N$[a)] | $g$-Value |
|---|---|---|---|
| Cyclohexane | 2.02 | 15.10 | 2.00610 |
| $CCl_4$ | 2.23 | 15.27 | 2.00607 |
| Benzene | 2.27 | 15.35 | 2.00603 |
| Toluene | 2.38 | 15.26 | 2.00603 |
| THF | 7.39 | 15.29 | 2.00604 |
| Acetone | 20.5 | 15.38 | 2.00599 |
| DMF | 36.7 | 15.57 | 2.00599 |
| $CH_3CN$ | 37.5 | 15.51 | 2.00595 |

a) hfcc of nitrogen in gauss.

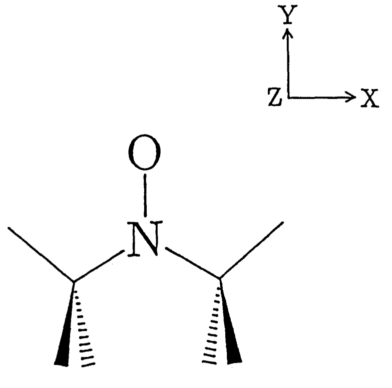

Fig. 1. DTBN model with $C_{2v}$ planar symmetry.

slightly less negative when $\varepsilon$ increases. Thus, DTBN is expected to be polarized in a polar solvent. The $\pi$ spin density on the nitrogen atom increases with an increase in $\varepsilon$ (Table 2). This elucidates well the observed solvent dependence of $a_N$, since it is propotional to the spin density of the 2s-atomic orbital of the nitrogen atom, which is generated by the spin-polarization mechanism.

Little attention has been paid to the solvent dependence of the $g$-value of a free radical. The present theoretical results reproduce well the solvent effect on the $g$-value of DTBN. In Table 3, three $g$-shifts are shown for $\varepsilon$=1 and for $\varepsilon$=40. From this table it is found that the $\Delta g_{yy}$ is dominant and that $\delta g_{yy}(12,13)$ makes the largest contribution to $\Delta g_{yy}$. The 13th MO is the singly-occupied MO (SOMO); the 12th MO corresponds the oxygen lone-pair orbital. Hence, $\Delta g_{yy}$ can be approximated by

$$\Delta g_{yy} \simeq \rho_\pi^{(O)}/\Delta E_{n\to\pi^*}. \qquad (13)$$

When $\varepsilon$ increases, $\rho_\pi^{(O)}$ decreases (Table 2), while $\Delta E_{n\to\pi^*}$ increases (Table 3). The tendency calculated for $\Delta E_{n\to\pi^*}$ has been observed in the visible spectra of DTBN in solution by Kawamura et al.[4] in which the $n\to\pi^*$ excitation energy increases with an increase in the solvent polarity. As a result, the observed solvent dependence of the $g$-value of DTBN is well elucidated by the present calculations.

**Galvinoxyl.** The solvent dependence of the $g$-value of galvinoxyl was found to be very small; MNDOS-CI calculations have shown that the $g$-value of galvinoxyl is almost constant. On the other hand, the hfcc of the methine proton and the ring protons of galvinoxyl decrease as $\varepsilon$ increases. Thus, the solvent dependence of hfcc of galvinoxyl was examined in some detail.

In the MO calculations, the $t$-butyl groups in galvinoxyl were replaced by hydrogen atoms. Four representative structures of galvinoxyl are shown in Fig. 2. The X-ray analysis has shown that the galvinoxyl has a $C_2$ twisted structure.[19] The UHF-MNDO calculation also supported the $C_2$ twisted structure as the lowest-energy structure (Table 5). Thus, the $C_2$ twisted structure was optimized by the RHF-MNDOS method for several $\varepsilon$ values, and the hfcc were obtained by RHF-MNDOS-CI calculations. The computational results are shown in Table 6. The hfcc of the methine proton

Table 2. Solvent Dependence of hfcc, $g$-Value, Atomic Charges, and $\pi$-Spin Densities for DTBN Model Calculated by RHF-MNDOS-CI Method

| $\varepsilon$ | $a_N$[a)] | $g$-value | $Q_N$ | $Q_O$ | $\rho_\pi^{(N)}$ | $\rho_\pi^{(O)}$ |
|---|---|---|---|---|---|---|
| 1.0 | 11.28 | 2.00628 | −0.1633 | −0.2586 | 0.3658 | 0.6059 |
| 2.0 | 12.58 | 2.00609 | −0.1826 | −0.3502 | 0.4169 | 0.5529 |
| 5.0 | 13.91 | 2.00582 | −0.1872 | −0.4472 | 0.4737 | 0.4924 |
| 10.0 | 14.50 | 2.00567 | −0.1846 | −0.4932 | 0.5009 | 0.4629 |
| 20.0 | 14.83 | 2.00559 | −0.1816 | −0.5198 | 0.5165 | 0.4458 |
| 40.0 | 15.01 | 2.00554 | −0.1802 | −0.5343 | 0.5250 | 0.4365 |

a) hfcc of nitrogen in gauss.

Table 3. Calculated $g$-Shifts of the DTBN Model

| $\varepsilon$ | $\Delta g_{xx}$ | $\Delta g_{yy}$ | $\Delta g_{zz}$ | $\delta g_{yy}(12,13)$ | $\Delta E_{n\to\pi^*}$ |
|---|---|---|---|---|---|
| 1.0 | 0.00126 | 0.01063 | 0.0 | 0.01156 | 1.986 |
| 40.0 | 0.00203 | 0.00763 | 0.0 | 0.00835 | 2.426 |

Table 4. Experimental hfcc and $g$-Value of Galvinoxyl in Various Solvents

| Solvent | $\varepsilon$ | $a_H(m)$[a)] | $a_H(r)$[b)] | $g$-Value |
|---|---|---|---|---|
| Cyclohexane | 2.02 | 6.02 | 1.40 | 2.00449 |
| $CCl_4$ | 2.23 | 5.96 | 1.40 | 2.00448 |
| Benzene | 2.27 | 5.99 | 1.38 | 2.00447 |
| Toluene | 2.38 | 5.83 | 1.36 | 2.00447 |
| $Et_2O$ | 4.22 | 5.85 | 1.41 | 2.00448 |
| THF | 7.39 | 5.99 | 1.35 | 2.00445 |
| Acetone | 20.5 | 5.85 | 1.35 | 2.00445 |
| DMF | 36.7 | 5.69 | 1.34 | 2.00445 |
| $CH_3CN$ | 37.5 | 5.76 | 1.35 | 2.00443 |

a) hfcc of methine proton in gauss. b) hfcc of ring proton in gauss.

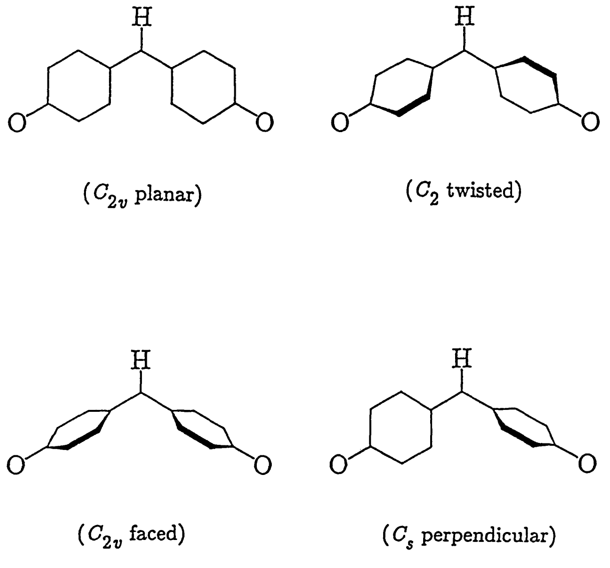

($C_{2v}$ planar) ($C_2$ twisted)

($C_{2v}$ faced) ($C_s$ perpendicular)

Fig. 2. Four representative structures of the galvinoxyl model.

Table 5. Calculated Total Energies (eV) and Relative Energies (kcal mol$^{-1}$) of Galvinoxyl[a)]

| Symmetry | State | RHF | | UHF | |
|---|---|---|---|---|---|
| | | Total | Rel | Total | Rel |
| $C_{2v}$ planar | $^2A_2$ | −2430.046 | 6.7 | −2431.112 | 2.5 |
| $C_2$ twisted | $^2A$ | −2430.096 | 5.5 | −2431.221 | 0.0 |
| $C_{2v}$ faced | $^2B_1$ | −2428.036 | 53.1 | ··· | |
| $C_s$ perpendicular | $^2A'$ | −2430.336 | 0.0[b)] | −2430.982 | 5.5 |

a) The molecular structure was optimized under each symmetric restriction. b) The lowest state was predicted by RHF calculation to be the A′ state. This may be due to the doublet instability.[20]

Table 6. The Proton hfcc and $\pi$-Spin Densities of the Galvinoxyl Model Calculated by RHF-MNDOS-CI Method

| $\varepsilon$ | $a_H(m)$[a] | $a_H(i)$[b] | $a_H(e)$[c] | $\rho_\pi^{(C)}$ | $\rho_\pi^{(O)}$ |
|---|---|---|---|---|---|
| 1.0 | 6.05 | 0.94 | 0.89 | −0.1446 | 0.0487 |
| 2.0 | 5.98 | 0.93 | 0.87 | −0.1439 | 0.0473 |
| 5.0 | 5.87 | 0.89 | 0.82 | −0.1420 | 0.0464 |
| 10.0 | 5.81 | 0.83 | 0.75 | −0.1399 | 0.0460 |
| 20.0 | 5.76 | 0.76 | 0.67 | −0.1380 | 0.0453 |
| 40.0 | 5.70 | 0.69 | 0.60 | −0.1364 | 0.0453 |

a) hfcc of methine proton in gauss. b) hfcc of interior ring proton in gauss. c) hfcc of exterior ring proton in gauss.

and two ring protons decrease with an increase in $\varepsilon$. These are the trends observed in experiment. The $\pi$ spin density of the methine carbon atom decreases with an increase in $\varepsilon$. This is the reason why the hfcc of the methine proton decreases when $\varepsilon$ increases.

In this paper, the effective charge model of the solvent effect was introduced into the open-shell RHF formalism and the CI calculations. The RHF-MNDOS-CI method, thus obtained, was used to evaluate the solvent effect on the ESR parameters of DTBN and galvinoxyl. The computational results well elucidated the observed solvent dependences of the hfcc and $g$-value of these radicals.

## References

1) A. H. Reddoch and S. Konishi, *J. Chem. Phys.*, **70**, 2121 (1979).

2) S. Kubota and Y. Ikegami, *J. Phys. Chem.*, **82**, 2739 (1978).

3) P. Ludwig, T. Layloff, and R. N. Adams, *J. Am. Chem. Soc.*, **86**, 2568 (1964).

4) T. Kawamura, S. Matsunami, and T. Yonezawa, *Bull. Chem. Soc. Jpn.*, **40**, 1111 (1967).

5) M. Born, *Z. Phys.*, **1**, 45 (1920).

6) G. Klopman, *Chem. Phys. Lett.*, **1**, 200 (1967).

7) O. Tapia, "Quantum Theory of Chemical Reactions," ed by R. Daudel, A. Pullman, L. Salem, and A. Veillard, Reidel, Dordrecht (1981), Vol. 2, p. 25.

8) R. Constanciel and R. Contreras, *Theor. Chim. Acta*, **65**, 1 (1984).

9) M. J. S. Dewar and W. Thiel, *J. Am. Chem. Soc.*, **99**, 4899, 4907 (1977).

10) T. Kozaki, K. Morihashi, and O. Kikuchi, *J. Mol. Struct.* (*Theochem.*), **168**, 265 (1988).

11) O. Kikuchi, T. Natui, and T. Kozaki, *J. Mol. Struct.* (*Theochem.*), **207**, 103 (1990).

12) T. Kozaki, K. Morihashi, and O. Kikuchi, *J. Am. Chem. Soc.*, **111**, 1547 (1989).

13) K. Morihashi, H. Takase, and O. Kikuchi, *Bull. Chem. Soc. Jpn.*, **63**, 2113 (1990).

14) G. J. Hoijtink, E. de Boer, P. H. van der Meij, and W. P. Weijland, *Recl. Trav. Chim. Pays-Bas*, **75**, 487 (1956).

15) O. Chalvet and I. Jano, *C. R. Acad. Sci. Paris*, **256**, 1867 (1964); I. Jano, *C. R. Acad. Soc. Paris*, **261**, 103 (1965).

16) K. Hirao and H. Nakatsuji, *J. Chem. Phys.*, **59**, 1457 (1973).

17) A. Carrington and A. D. McLachlan, "Introduction to Magnetic Resonance," Harper and Row, New York (1967).

18) A. J. Stone, *Proc. Roy. Soc. A*, **271**, 424 (1963).

19) D. E. Williams, *Mol. Phys.*, **16**, 145 (1969).

20) O. Kikuchi, *Chem. Phys. Lett.*, **72**, 487 (1980), and references cited therein.